JOURNAL OF SPACECRAFT AND ROCKETS
Vol. 42, No. 5, September–October 2005

Engineering Notes

ENGINEERING NOTES are short manuscripts describing new developments or important results of a preliminary nature. These Notes should not exceed 2500 words (where a figure or table counts as 200 words). Following informal review by the Editors, they may be published within a few months of the date of receipt. Style requirements are the same as for regular contributions (see inside back cover).

Near-Optimal Solar-Sail Orbit-Raising from Low Earth Orbit

Giovanni Mengali* and Alessandro A. Quarta†
University of Pisa, I-56122 Pisa, Italy

Introduction

SOLAR-SAIL technology has attracted the interest of the scientific community as an advanced propulsion means capable of promoting the reduction of mission costs, the increase of payload mass fraction, and the feasibility of missions that are not practically accessible via conventional propulsion because of their large ΔV requirements.

Optimal solar-sail trajectories have long been investigated because of their importance for practical mission analysis purposes.[1] Although globally optimal trajectories are especially well suited for interplanetary missions, there are many instances where different engineering constraints limit the possibility of using optimal steering laws. Accordingly, simpler maneuver strategies are required. This happens in most planet-centered problems, including orbit-raising and Earth-escape trajectories. In these cases suboptimal (or locally optimal) control laws that maximize the instantaneous rate of change of a particular orbital element or another scalar function of the orbital elements are often employed. This approach not only provides simple answers to the designer, but also gives steering laws that, in many cases, are close to minimum-time solutions. For these reasons, locally optimal control laws for ideal sails have been studied in various forms with different perturbation models.

In most papers available in the literature,[2–7] the simplifying assumption of neglecting the aerodynamic drag is made. Although the aerodynamic drag has been sometimes taken into account in the mission analysis,[8,9] no systematic study concerning its effects on the solar-sail trajectories is currently available.

Air drag is known to be negligible above 1000 km, even if its effects are strongly influenced by the solar activity. Nevertheless, air drag can become important as long as particular maneuvers, such as orbit raising from low Earth orbit, are concerned. Accordingly, in this Note we analyze the effects of air drag on sail trajectories in a systematic way, deriving a locally optimal steering law that takes a suitable aerodynamic model into account. To this end, the sail is treated as a flat plate, and a hyperthermal flow model is assumed. The corresponding trajectories are near-minimum-time solutions for low characteristic accelerations. The steering law is shown to depend on the ratio between the local dynamic pressure and the solar radiation pressure on the sail. A case study is presented, where the steering law is applied to investigate the orbit-raising and Earth-escape problems.

Received 25 October 2004; revision received 2 March 2005; accepted for publication 24 March 2005.

*Associate Professor, Department of Aerospace Engineering; g.mengali@ing.unipi.it.
†Research Assistant, Department of Aerospace Engineering; a.quarta@ing.unipi.it.

Mathematical Model

The equations of motion for a flat ideal solar sail with mass m and area A in a geocentric inertial frame $\mathcal{T}_\oplus(x, y, z)$ are given by

$$\dot{\boldsymbol{r}} = \boldsymbol{v} \tag{1}$$

$$\dot{\boldsymbol{v}} = -\left(\mu_\oplus / r^3\right)\boldsymbol{r} + (P_\oplus A/m)(\hat{\boldsymbol{r}}_{\odot s} \cdot \hat{\boldsymbol{n}})^2 \hat{n} + \boldsymbol{a}_d + \boldsymbol{a}_p \tag{2}$$

where $[\boldsymbol{r}]_{\mathcal{T}_\oplus} = [r_x, r_y, r_z]^T$ and $[\boldsymbol{v}]_{\mathcal{T}_\oplus} = [v_x, v_y, v_z]^T$ are the position and velocity vectors of the spacecraft relative to $\mathcal{T}_\oplus$, with $r \triangleq \|\boldsymbol{r}\|$ and $v \triangleq \|\boldsymbol{v}\|$, $\boldsymbol{a}_d$ is the aerodynamic acceleration and $\boldsymbol{a}_p$ is the total disturbing acceleration, which does not depend on the solar-sail attitude. Also, $\mu_\oplus$ is the Earth's gravitational parameter, $\hat{\boldsymbol{r}}_{\odot s}$ is the sun-sail unit vector, $\hat{\boldsymbol{n}}$ is the unit vector normal to the sail in the direction of thrust, and $P_\oplus$ is the solar radiation pressure (function of the spacecraft distance from the sun) for a perfectly reflecting sail. A mean value for $P_\oplus$ is 9.114×10^{-6} Pa for a sail in Earth orbit.

For mathematical convenience the solar sail is modeled as a flat plate,[9] and the aerodynamic acceleration is given by

$$\boldsymbol{a}_d = (1/2m)\rho A v^2 (C_L \hat{\boldsymbol{v}}_\perp - C_D \hat{\boldsymbol{v}}) \tag{3}$$

where ρ is the local atmospheric density,[10] C_L and C_D are the lift and drag coefficients, and $\hat{\boldsymbol{v}}_\perp$ is the unit vector perpendicular to $\hat{\boldsymbol{v}}$ in the plane $(\hat{\boldsymbol{v}}, \hat{\boldsymbol{n}})$. Assuming a hyperthermal flow, that is, translational velocity of the solar sail much larger than the thermal velocities of the atmospheric particles, the lift and drag coefficients are[11,12]

$$C_L = 2[(2 - \sigma_n - \sigma_t)\cos\zeta + \sigma_n (v_b/v)]\sin\zeta\cos\zeta \tag{4}$$

$$C_D = 2\left[(2 - \sigma_n - \sigma_t)\cos^2\zeta + \sigma_n (v_b/v)\cos\zeta + \sigma_t\right]\cos\zeta \tag{5}$$

where σ_n and σ_t are the accommodation coefficients for normal and tangential momentum exchange, v_b is the mean thermal speed of an atmospheric particle at the temperature of the sail, and $\zeta \in [0, \pi/2]$ is the angle between $\hat{\boldsymbol{v}}$ and $\hat{\boldsymbol{n}}$, namely,

$$\cos\zeta \triangleq \hat{\boldsymbol{v}} \cdot \hat{\boldsymbol{n}} \tag{6}$$

Clearly, ζ is complementary of the conventional angle of attack for a flat plate. Note that at the altitudes of interest[9] the term v_b/v in Eq. (5) is typically about 0.05.

Let $\mathcal{T}_{\text{orb}}(x_{\text{orb}}, y_{\text{orb}}, z_{\text{orb}})$ be an orbital frame whose unit vectors are $\hat{\boldsymbol{i}}_{\text{orb}} \equiv \hat{\boldsymbol{r}}_{\odot s}$, $\hat{\boldsymbol{j}}_{\text{orb}}$, and $\hat{\boldsymbol{k}}_{\text{orb}}$. Assume that the plane $z_{\text{orb}} = 0$ contains the axis z of the $T_\oplus$ frame and y_{orb} points toward the Earth's north pole. Introducing the sail clock angle $\delta \in [-\pi, \pi]$ (Fig. 1), and the sail cone angle $\alpha \in [0, \pi/2]$ defined as

$$\alpha \triangleq \cos^{-1}(\hat{\boldsymbol{r}}_{\odot s} \cdot \hat{\boldsymbol{n}}) \tag{7}$$

the components of $\hat{\boldsymbol{n}}$ and $\hat{\boldsymbol{v}}$ can be expressed in the $\mathcal{T}_{\text{orb}}$ frame as

$$[\hat{\boldsymbol{n}}]_{\mathcal{T}_{\text{orb}}} = [\cos\alpha, \sin\alpha\cos\delta, \sin\alpha\sin\delta]^T \tag{8}$$

$$[\hat{\boldsymbol{v}}]_{\mathcal{T}_{\text{orb}}} = [\cos\alpha_v, \sin\alpha_v\cos\delta_v, \sin\alpha_v\sin\delta_v]^T \tag{9}$$

Problem Statement

An efficient method for orbit raising is to use a locally optimal steering law that maximizes the instantaneous rate of change of

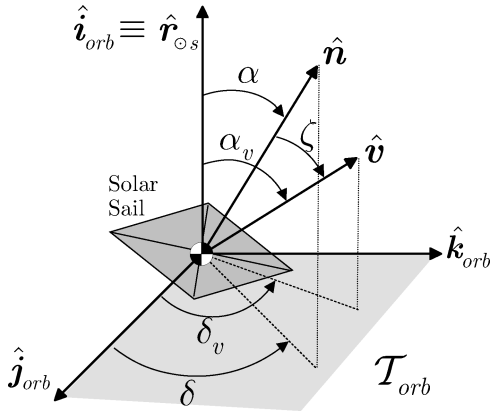

Fig. 1 Orbital frame and solar-sail angles.

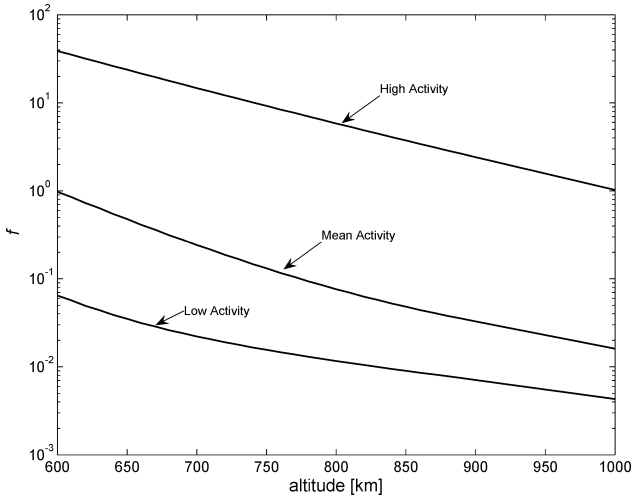

Fig. 2 Variation of f with the altitude and the solar activity ($P_\oplus \cong 9.114 \times 10^{-6}$ Pa).

the solar-sail semimajor axis at all points along the trajectory. It is well known[1,4] that this control law is identical to locally maximizing the instantaneous rate of change of the orbital specific energy $\varepsilon = \frac{1}{2}\boldsymbol{v}\cdot\boldsymbol{v} - \mu_\oplus/r$. Coverstone and Prussing[6] have applied this latter strategy to reach an escape condition from the Earth using a solar sail. It can be shown[6] that the corresponding trajectories are near-minimum-time solutions as long as typical sail accelerations (on the order of $10^{-4}g$ or less) are considered. Here we revisit the problem of maximizing the energy gain including the effect of the aerodynamic force.

Taking the scalar product of the equation of motion (2) with the solar-sail velocity vector $\boldsymbol{v}$ and using Eqs. (3) and (7) yields

$$\dot{\varepsilon} = \boldsymbol{a}_p \cdot \boldsymbol{v} + (P_\oplus A/m) v \cos^2\alpha(\hat{\boldsymbol{n}}\cdot\hat{\boldsymbol{v}}) - (1/2m)\rho\, A\, C_D v^3 \qquad (10)$$

When angle ζ [see Eq. (6)] is inserted into Eq. (10), the rate of change of the specific energy becomes

$$\dot{\varepsilon} = \boldsymbol{a}_p \cdot \boldsymbol{v} + (P_\oplus A/m) v\left[\cos^2\alpha\cos\zeta - f(C_D/2)\right] \qquad (11)$$

where

$$f \triangleq \rho v^2 \big/ P_\oplus \qquad (12)$$

By definition, the nondimensional variable $f \geq 0$ equals twice the ratio of the local dynamic pressure $(\rho v^2/2)$ to the solar radiation pressure on the ideal sail $(P_\oplus)$. For near-circular orbits $v^2 \cong \mu_\oplus/r$, hence

$$f \cong \mu_\oplus\, \rho/(P_\oplus\, r) \qquad (13)$$

In other terms, f is a function of the solar-sail altitude and the solar activity (Fig. 2). Note that f can be used to estimate the minimum altitude at which a solar-sail spacecraft can operate. Indeed, imposing the condition that the maximum sail thrust is balanced against the maximum aerodynamic drag provides

$$P_\oplus A = \rho A v^2 C_{D_{\max}} \big/ 2 \qquad (14)$$

from which $f C_{D_{\max}}/2 = 1$. Assuming $C_{D_{\max}} \cong 2$, the minimum operating altitude for a solar sail is achieved for $f = 1$. Figure 2 shows that the minimum operating altitude is about 1000 and 600 km for high and medium solar activity, respectively. These results are in agreement with the previous values found in the literature.[9] Finally, f plays a fundamental role in the steering law, as discussed later.

As mentioned before, the problem is that of finding the control law $\boldsymbol{u}(t) = [\alpha(t),\ \delta(t)]^T$, which, at any given time, maximizes $\dot{\varepsilon}$. This amounts to maximizing the performance index J, which coincides with that portion of the function $\dot{\varepsilon}$ that explicitly depends on the control vector, that is,

$$\boldsymbol{u} = \arg\max_{u\,\in\,\mathcal{U}} J \qquad (15)$$

where $\mathcal{U}$ is the domain of feasible controls and

$$J \triangleq \dot{\varepsilon} - \boldsymbol{a}_p \cdot \boldsymbol{v} = (P_\oplus A/m) v\left[\cos^2\alpha\cos\zeta - f(C_D/2)\right] \qquad (16)$$

Substituting Eqs. (5) and (12) into (16) yields

$$J = \Big\{(P_\oplus A v/m)\cos^2\alpha - (\rho v^3 A/m)\Big[(2-\sigma_n-\sigma_t)\cos^2\zeta + \sigma_n(v_b/v)\cos\zeta + \sigma_t\Big]\Big\}\cos\zeta \qquad (17)$$

Near-Optimal Control Law

Invoking the necessary condition $\partial J/\partial\delta = 0$ to maximize J and taking into account Eqs. (6), (8), and (9), it is found that

$$\tan\delta = \tan\delta_v \qquad (18)$$

Equation (18) implies that the unit vectors $\hat{\boldsymbol{\imath}}_{\rm orb}$, $\hat{\boldsymbol{v}}$, and $\hat{\boldsymbol{n}}$ are coplanar. Accordingly, from Fig. 1 one has

$$\cos\zeta = \cos(\alpha_v - \alpha) \qquad (19)$$

This allows one to remove the dependence on ζ in the performance index J. The other necessary condition to maximize J is given by $\partial J/\partial\alpha = 0$. Substituting Eq. (19) into (17) yields the following nonlinear equation:

$$-\cos\alpha[2\sin\alpha\cos(\alpha-\alpha_v) + \cos\alpha\sin(\alpha-\alpha_v)] + f\sin(\alpha-\alpha_v)\Big[3(2-\sigma_n-\sigma_t)\cos^2(\alpha-\alpha_v) + 2\sigma_n(v_b/v)\cos(\alpha-\alpha_v) + \sigma_t\Big] = 0 \qquad (20)$$

Once solved numerically, Eq. (20) provides the values of the sail cone angle that render the functional J stationary. Of course, these values are a function of the velocity cone angle α_v, the aerothermodynamic sail properties σ_n, σ_t, and v_b/v, and the variable f. In particular, when $f = 0$, which corresponds to neglecting the aerodynamic drag, Eq. (20) can be solved in closed form and gives the well-known near-optimal steering law for an ideal sail with no external perturbations[1,4]:

$$\alpha_{(f=0)} = \tan^{-1}\left(\frac{-3\cos\alpha_v + \sqrt{8+\cos^2\alpha_v}}{4\sin\alpha_v}\right) \qquad (21)$$

Suppose now $f \neq 0$. Note that a generic point (α, α_v) solution of Eq. (20) is a maximum for J provided that $J(\alpha, \alpha_v) \geq 0$. The set $\mathcal{S}$ of points that maximize J, that is, $\mathcal{S} = \{\partial J/\partial\alpha = 0 \cap J \geq 0\}$, is represented in Fig. 3 for different values of f. A point belonging to $\mathcal{S}$ will be referred to as $(\tilde{\alpha}, \tilde{\alpha}_v)$. Figure 3 shows that the regions of the plane (α, α_v), where J is positive, tend to become smaller and smaller as f increases. Note that $\mathcal{S}$ contains the point $P^* \equiv (\alpha^*, \alpha_v^*)$

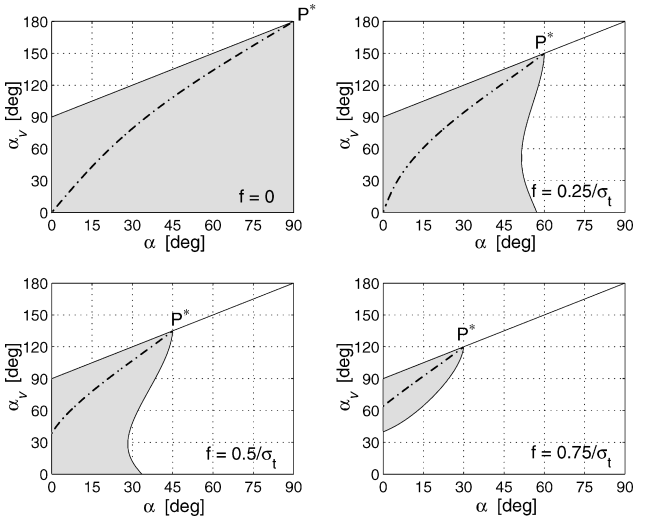

Fig. 3 Regions of the plane (α, α_v), where $J = 0$ (——), $J > 0$ (in gray), and corresponding maxima of J (set $\mathcal{S}$, –·–·–) for different values of f.

in which both conditions $\partial J/\partial\alpha = 0$ and $J = 0$ are met. This point can be found observing that $\cos\zeta = 0$ implies $C_D = 0$ and, hence, $J = 0$ [see Eqs. (5) and (16)]. In other terms, equation $J = 0$ is satisfied by the pairs (α, α_v) such that

$$\alpha = \alpha_v - \pi/2 \tag{22}$$

Substituting Eq. (22) into (20) and solving for α provides the value $\alpha = \alpha^*$, which nullifies both J and $\partial J/\partial\alpha$. The result is

$$\alpha^* = \cos^{-1}\sqrt{f\sigma_t} \tag{23}$$

from which

$$\alpha_v^* = \alpha^* + \pi/2 \tag{24}$$

The presence of a critical point P^* has a clear physical interpretation. Indeed, the functional J is the sum of the specific power caused by the solar sail (which is positive) and the specific power caused by the atmospheric drag (which is negative by definition). When $\alpha > \alpha^*$, the modulus of the power caused by the drag is greater than the propulsive power. In this latter case $\dot{\varepsilon}$ can be maximized only through that particular value of the cone angle for which $J = 0$.

Note that the values of the cone angle solutions of Eq. (20) can be negative. However, these solutions are outside the admissible interval of variation for α. This happens whenever the set $\mathcal{S}$ contains the point $P_0 \equiv (0, \alpha_{v_0})$, with $\alpha_{v_0} > 0$. To find when such a situation occurs, substitute $\alpha = 0$ into Eq. (20). In doing so the following second-order polynomial equation in $\cos\alpha_{v_0}$ is obtained:

$$3f(2-\sigma_n-\sigma_t)\cos^2\alpha_{v_0} + 2f\sigma_n(v_b/v)\cos\alpha_{v_0} + f\sigma_t - 1 = 0 \tag{25}$$

which must be solved for α_{v_0}. A solution exists in the range $\alpha_{v_0} \in (0, \pi/2)$ provided that $0 < h < 1$, where

$$h \triangleq \frac{-f\sigma_n v_b/v + \sqrt{(f\sigma_n v_b/v)^2 + 3f(1-f\sigma_t)(2-\sigma_n-\sigma_t)}}{3f(2-\sigma_n-\sigma_t)} \tag{26}$$

and $\alpha_{v_0} = \cos^{-1} h$. Note that Eq. (26) is a function of the variable f. Accordingly, setting $h = 1$ and 0 respectively provides the minimum f_1 and maximum f_2 value of f satisfying the inequality $0 < h < 1$. The results are

$$f_1 = 1/\{\sigma_t[3(2/\sigma_t - \sigma_n/\sigma_t - 1) + 2(\sigma_n/\sigma_t)(v_b/v) + 1]\} \tag{27}$$

$$f_2 = 1/\sigma_t \tag{28}$$

It can be easily verified that, as long as $0 < h < 1$, the maximum of J is given by $J(0, \alpha_{v_0})$.

To summarize, recalling that $\tilde{\alpha}$ is a solution of Eq. (20) constrained by $J \geq 0$, it is useful to distinguish between three cases for defining the steering law maximizing J.

Case 1: $0 \leq f < f_1$

$$\alpha = \begin{cases} \tilde{\alpha} & \text{if} \quad 0 \leq \alpha_v < \alpha_v^* \\ \alpha_v - \pi/2 & \text{if} \quad \alpha_v > \alpha_v^* \end{cases} \tag{29}$$

Case 2: $f_1 \leq f \leq f_2$

$$\alpha = \begin{cases} 0 & \text{if} \quad 0 \leq \alpha_v \leq \cos^{-1} h \\ \tilde{\alpha} & \text{if} \quad \cos^{-1} h < \alpha_v < \alpha_v^* \\ \alpha_v - \pi/2 & \text{if} \quad \alpha_v > \alpha_v^* \end{cases} \tag{30}$$

Case 3: $f > f_2$

$$\alpha = \begin{cases} 0 & \text{if} \quad 0 \leq \alpha_v \leq \pi/2 \\ \alpha_v - \pi/2 & \text{if} \quad \alpha_v > \pi/2 \end{cases} \tag{31}$$

Note that case 3 is of no practical interest. Indeed, because σ_t is typically in the range [0.8, 0.9] (Ref. 11), Eq. (28) implies $f_2 > 1$. As already shown, this would correspond to a situation where the solar sail is below the minimum operating altitude. Note also that the steering law is consistent with the absence of aerodynamic drag. In fact $f = 0$ (that is, $C_D = 0$) implies $\alpha^* = \pi/2$ (see Fig. 3), which corresponds to the maximum value admissible for α. In other terms the control law (29) coincides, over the whole interval of variation of α, with the solutions of Eq. (20), which, in turn, are given by Eq. (21).

Numerical Simulations

The steering law described earlier was applied to investigate the problem of orbit raising for an ideal solar-sail spacecraft. The equations of motion (1) and (2) have been integrated in double precision using a variable-order Adams–Bashforth–Moulton solver[13] with absolute and relative errors of 10^{-10}. A set of canonical units[14] $DU_\oplus \triangleq 6378.13655$ km and $TU_\oplus \triangleq 806.81103s(\mu_\oplus = 1\ DU_\oplus^3/TU_\oplus^2)$ has been used to reduce the numerical sensitivity of the differential problem. The perturbing acceleration $\boldsymbol{a}_p$ includes the lunisolar gravitational attraction[15] and the Earth oblateness effects[16] (up to J_6). The geocentric ephemeris for the sun and the moon are based on the Jet Propulsion Laboratory DE200/LE200 model.[17,18] This allows one to take into account the time variation in the magnitude of the solar flux (about 6% in one year) because of the Earth's orbit eccentricity.

To avoid the problem of Earth's shadow,[9] an initial sun-synchronous circular orbit is assumed for the solar sail. The parking orbit has an altitude of 650 km, an inclination of 96.6 deg, and a right ascension of the ascending node such as to maximize the orbital plane illumination caused by the sun. Note that the orbital altitude is compatible with the minimum operating altitude (approximately 600 km) for an ideal sail under mean conditions of solar and geomagnetic activities (see Fig. 2). The accommodation coefficients for normal and tangential momentum exchange are $\sigma_n = \sigma_t = 0.8$.[11]

The problem of doubling the distance of the spacecraft from the Earth using the control laws (29–31) has been investigated. Simulations indicate that the deployment date has a negligible effect on the mission times. This conclusion is in agreement with previous studies.[6,19] Accordingly, a starting date of 21 March 2005 has been used in the simulations, and an initial longitude of the ascending node of 90 deg has been assumed. The problem has been first solved for the ideal case of absence of atmospheric drag (that is, $f = 0$), using different characteristic accelerations a_c in the range [0.1, 2] mm/s^2. The corresponding mission times, referred to as Δt_i, are shown in Fig. 4. Then, a time comparison has been made with the inclusion of the atmospheric drag in the simulations. Two cases have been investigated. In case 1 the near-optimal steering law (29–31) has been applied. In addition (case 2), a set of simulations have been run using the ideal control law (21) with the inclusion

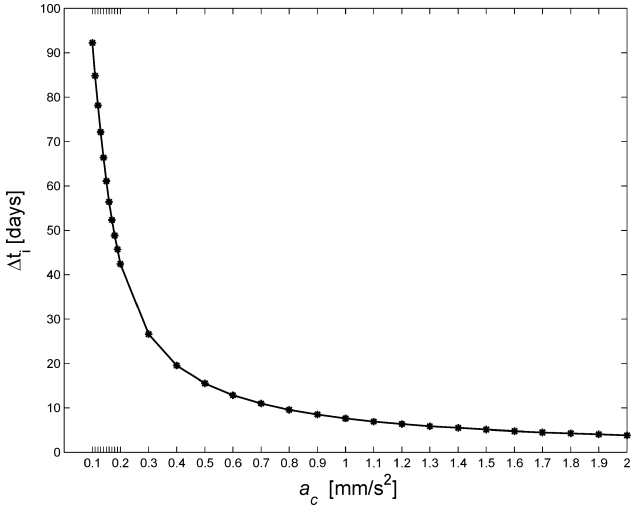

Fig. 4 Time to double the initial sail altitude neglecting the atmospheric drag.

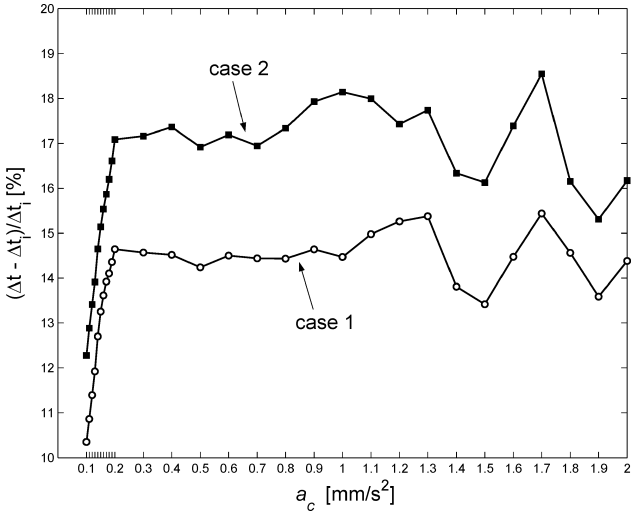

Fig. 5 Time to double the initial sail altitude using the control law (29–31) (○, case 1) and using the ideal control law (21) with the inclusion of drag in the simulations (■, case 2).

of the atmospheric drag (that is, $\boldsymbol{a}_d \neq 0$ in the equation of motion). Figure 5 shows the percentage increase in mission times with respect to the case of absence of atmospheric drag. For both cases 1 and 2, the percentage increase in mission times is significant in all of the range of characteristic accelerations. As expected, case 2 (which is not near optimal) behaves worse than the near-optimal control law (case 1). Finally, assuming $a_c = 1$ mm/s^2, Fig. 6 shows the remarkable differences between the time histories of the sail cone angles obtained from the near-optimal steering law with and without the inclusion of the atmospheric drag (that is, letting $f \neq 0$ and $f = 0$, respectively).

Because the steering law (29–31) locally maximizes the instantaneous rate of change of the orbital specific energy, it can be applied also for studying the problem of Earth escape from low Earth orbit. However, the inclusion of the atmospheric drag in the model has a negligible effect on the escape times. The reason is that the sail operates for most of the time in conditions characterized by very low air density, that is, $f \cong 0$. This is confirmed by Fig. 7, where the variable f is plotted as a function of time. Figure 7 shows that f is significantly different from zero only for t less than about 15 days, whereas the time to escape is 204 days.

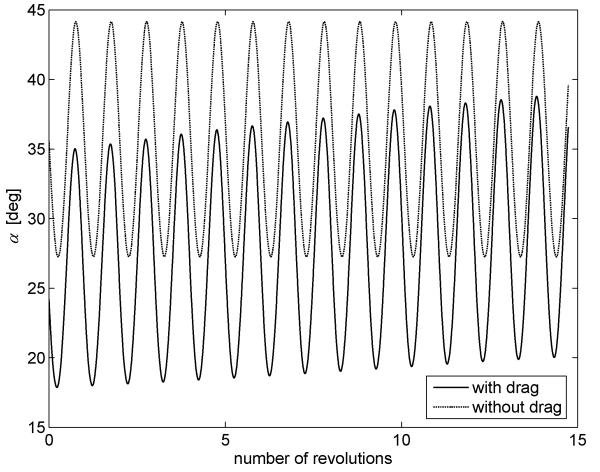

Fig. 6 Time histories of the sail cone angle corresponding to the near-optimal steering law with and without the inclusion of the atmospheric drag ($a_c = 1$ mm/s^2).

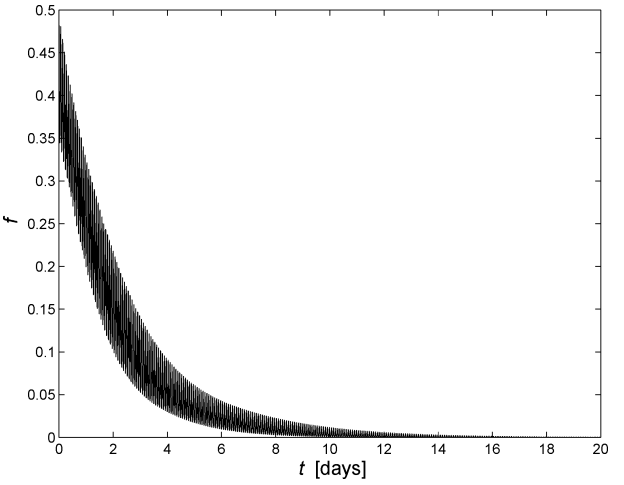

Fig. 7 Time history of variable f in Earth-escape problem ($a_c = 1$ mm/s^2).

Conclusions

The problem of orbit raising from low Earth orbit by using an ideal solar sail has been investigated. The equations of motion include the effect of the air drag. The sail is modeled as a flat plate, and a hyperthermal flow around the spacecraft is assumed. The analysis is made in a systematic way through a near-optimal formulation. In fact, the problem is translated into that of finding the steering law that maximizes the instantaneous rate of change of the solar-sail semimajor axis along all points of the trajectory. The resulting steering law is shown to depend on the air drag through the ratio between the local dynamic pressure and the solar radiation pressure on the sail. Extensive numerical simulations have been run to compare the new steering law with others available in the literature when neglecting the drag effect. Not only are there remarkable differences between the time histories of the sail cone angle when air drag is taken into account, but also the effects over the mission times are significant.

References

[1]McInnes, C. R., *Solar Sailing: Technology, Dynamics and Mission Applications*, Springer-Praxis Series in Space Science and Technology, Springer-Verlag, Berlin, 1999, pp. 113–170.

[2]Sackett, L. L., and Edelbaum, T. N., "Optimal Solar Sail Spiral to Escape," American Astronautical Society and AIAA, Paper A78 31-901, Sept. 1977.

[3]Fekete, T. A., Sackett, L. L., and von Flotow, A. H., "Trajectory Design for Solar Sailing from Low-Earth Orbit to the Moon," *Advances in the Astronautical Sciences*, Vol. 79, Feb. 1992, pp. 1083–1094.

[4]Macdonald, M., and McInnes, C. R., "Analytic Control Laws for Near-Optimal Geocentric Solar Sail Transfers," American Astronautical Society, Paper 01-472, July–Aug. 2001.

[5]Leipold, M., "Solar Sail Mission Design," Ph.D. Dissertation, Technische Univ. München, DLR FB 2000 22, Munich, Feb. 2000.

[6]Coverstone, V. L., and Prussing, J. E., "Technique for Escape from Geosynchronous Transfer Orbit Using a Solar Sail," *Journal of Guidance, Control, and Dynamics*, Vol. 26, No. 4, 2003, pp. 628–634.

[7]Mengali, G., and Quarta, A. A., "Earth Escape by Ideal Sail and Solar-Photon Thrustor Spacecraft," *Journal of Guidance, Control, and Dynamics*, Vol. 27, No. 6, 2004, pp. 1105–1108.

[8]Leipold, M., Garner, C. E., Freeland, R., Herrmann, A., Noca, M., Pagel, G., Seboldt, W., Sprague, G., and Unckenbold, W., "ODISSEE—A Proposal for Demonstration of a Solar Sail in Earth Orbit," *Acta Astronautica*, Vol. 45, No. 4–9, 1999, pp. 557–566.

[9]Fieseler, P. D., "A Method for Solar Sailing in a Low Earth Orbit," *Acta Astronautica*, Vol. 43, No. 9–10, 1998, pp. 531–541.

[10]Hedin, A. E., "Extension of the MSIS Thermosphere Model into the Middle and Lower Atmosphere," *Journal of Geophysical Research*, Vol. 96, No. A2, 1991, pp. 1159–1172.

[11]Hughes, P. C., *Spacecraft Attitude Dynamics*, Wiley, New York, 1986, pp. 248–280.

[12]NASA Space Vehicle Design Criteria, "Spacecraft Aerodynamic Torques," NASA SP-8058, Jan. 1971.

[13]Shampine, L. F., and Reichelt, M. W., "The MATLAB ODE Suite," *SIAM Journal on Scientific Computing*, Vol. 18, No. 1, 1997, pp. 1–22.

[14]Standish, E. M., "Report of the IAU WGAS Sub-Group on Numerical Standards," IAU Working Group on Astronomical Standards, Tech. Rept. [online report], URL: http://ssd.jpl.nasa.gov/iau-comm4/iausgnsrpt.ps [cited 1 March 2005].

[15]Battin, R. H., *An Introduction to the Mathematics and Methods of Astrodynamics*, AIAA Education Series, AIAA, New York, 1987, pp. 387–391.

[16]Roy, A. E., *Orbital Motion*, 3rd ed., Advances in Design and Control, Inst. of Physics Publishing, Bristol, England, U.K., 1988, pp. 511, 512.

[17]Standish, E. M., "Orientation of the JPL Ephemerides, DE200/LE200, to the Dynamical Equinox of J2000," *Astronomy and Astrophysics*, Vol. 114, No. 2, 1982, pp. 297–302.

[18]Standish, E. M., "The Observational Basis for JPL's DE200, the Planetary Ephemerides of the Astronomical Almanac," *Astronomy and Astrophysics*, Vol. 233, No. 1, 1990, pp. 252–271.

[19]Macdonald, M., and McInnes, C. R., "Seasonal Efficiencies of Solar Sailing in Planetary Orbit," International Astronautical Congress, Paper 02-S.6.01, Oct. 2002.

D. Spencer
Associate Editor